

# Global fermionic mode optimization via swap gates

Gero Friesecke,<sup>1,\*</sup> Miklós Antal Werner,<sup>2</sup> Kornél Kapás,<sup>2,3</sup> Andor Menczer,<sup>2</sup> and Örs Legeza<sup>2,4,†</sup>

<sup>1</sup>*Department of Mathematics, Technical University of Munich, Germany*

<sup>2</sup>*Strongly Correlated Systems Lendület Research Group,*

*Wigner Research Centre for Physics, H-1525, Budapest, Hungary*

<sup>3</sup>*Department of Theoretical Physics, Institute of Physics,*

*Budapest University of Technology and Economics, Műegyetem rkp. 3, H-1111 Budapest, Hungary*

<sup>4</sup>*Institute for Advanced Study, Technical University of Munich, Germany, Lichtenbergstrasse 2a, 85748 Garching, Germany*

(Dated: June 6, 2024)

We propose a general approach to find an optimal representation of a quantum many body wave function for a given error margin via global fermionic mode optimization. The stationary point on a fixed rank matrix product state manifold is obtained via a joint optimization on the Grassman manifold [Phys. Rev. Lett. 117, 210402] together with swap gates controlled permutations. The minimization of the global quantity, the block entropy area, guarantees that the method fulfills all criteria with respect to partial derivatives. Numerical results via large scale density matrix renormalization group simulations on strongly correlated molecular systems and two-dimensional fermionic lattice models are discussed.

*Introduction:* Finding an optimal representation of a quantum many body wave function, i.e., a parametrization with the minimum number of parameters for a given error margin is a task of utmost importance in modern quantum physics and chemistry [1–5]. Tensor network state (TNS) methods [6–9] building on the seminal work of S. R. White [10] provide an efficient tool to reduce the computational cost to a polynomial form. These standard approaches are, however, far from being optimal for systems of indistinguishable particles as they do not take into account the large freedom provided by the group of global one-particle rotations that can bring the representation much closer to the optimum [11–16].

For the one dimensional tensor topology, i.e., for the density matrix renormalization group (DMRG) method, the efficiency is determined by the entanglement scaling law [17, 18]. The iterative optimization of the parameters of the underlying matrix product state (MPS) wave function for a problem of  $N$  modes is performed by a sequence of local optimization steps based on singular value decomposition together with a truncation by keeping matrix ranks or the truncation error below a priorly given threshold. Therefore, the computational complexity of a single optimization step is determined by the tail behavior of the associated Schmidt values. A good measure for this behaviour is the so-called block entropy. The sum of it over all bonds therefore indicates the total computational complexity of the whole sequence (sweep) and we will refer to it as the block entropy area (BEA). When mode optimization is also utilized, the  $N \times N$  dimensional matrix of the global unitary leads to a stationary point if the full derivative is zero which ultimately requires that all partial derivatives for each pairwise elements are also zero.

In our previous approach [12] we applied such pairwise optimization based on the reduction of the Rényi entropy of parameter  $\frac{1}{2}$  via nearest neighbor two-mode gates for a full sweep followed by global reordering of the modes based on the Fiedler-vector method [19]. This, however, neither guarantees that all pairwise elements are accessed via the optimization protocol, nor leads to a monotonically decreasing cost function. On the other hand, when energy gradient based optimization protocols are applied [11], for example, by replacing the CI solver in the complete active space self consistent field (CASSCF) procedure with DMRG [20], first it is not clear that the entanglement of the MPS is reduced and second a very high accuracy demand must be enforced on the DMRG to calculate the one- and two-particle reduced density matrices [21] which makes this procedure very costly.

In this work, we propose a general approach to obtain a stationary point on a fixed rank MPS manifold via a joint optimization on the Grassman manifold together with swap gates controlled permutations, aimed at simultaneously achieving low energy and low entanglement. The mode optimization is based on the minimization of the global quantity BEA, that we analyze analytically and also numerically via large scale DMRG simulations.

*Block entropy area:* As always in TNS methods, fermionic wavefunctions belonging to the Fock space over  $N$  single-particle modes  $\varphi_1, \dots, \varphi_N$  are represented via their coefficient tensor  $C(\mu_1, \dots, \mu_N)$  in the expansion

$$\Psi = \sum_{\mu_1, \dots, \mu_N=0}^1 C(\mu_1, \dots, \mu_N) \Phi_{\mu_1, \dots, \mu_N}$$

where the many-body basis functions are given by Slater determinants in the occupation representation,  $\Phi_{\mu_1 \dots \mu_N} := |\varphi_{i_1} \dots \varphi_{i_n}\rangle$  if  $\mu_i = 1$  exactly when  $i \in \{i_1, \dots, i_n\}$ ,  $i_1 < \dots < i_n$ . We introduce the block en-

\* gf@ma.tum.de

† legeza.ors@wigner.hu

tropy area (BEA)

$$\mathcal{B}_\alpha(C) = \sum_{\ell=1}^{N-1} S_\alpha(\rho_{1,2,\dots,\ell}) \quad (1)$$

where  $\rho_{1,2,\dots,\ell}$  is the reduced density operator of the first  $\ell$  modes,

$$\begin{aligned} & \rho_{1,2,\dots,\ell}(\mu_1, \dots, \mu_\ell; \mu'_1, \dots, \mu'_\ell) \\ &= \sum_{\mu_{\ell+1}, \dots, \mu_N} C(\mu_1, \dots, \mu_N) C^*(\mu'_1, \dots, \mu'_\ell, \mu_{\ell+1}, \dots, \mu_N) \end{aligned}$$

and  $S_\alpha$  is the Rényi entropy  $S_\alpha(\rho) = \frac{1}{1-\alpha} \ln(\text{Tr} \rho^\alpha)$  for some  $0 < \alpha < 1$ . (The word area is explained in Fig. 4.) One could also use the von Neumann entropy  $S_1(\rho) = \lim_{\alpha \rightarrow 1} \frac{1}{1-\alpha} \ln(\text{Tr} \rho^\alpha) = -\text{Tr} \rho \ln \rho$ . The important feature needed is concavity, so that density operators are favoured whose eigenvalues are either very large or very small. In practice we use the Rényi entropy with  $\alpha = 1/2$  for the optimization procedure. The block entropy area is a global quantity measuring the complexity of the coefficient tensor  $C$ , and strongly depends on the chosen basis. The proposal of this paper is to therefore use it as a target which should be optimized over fermionic mode transformations.

*Fermionic mode optimization:* Under a single particle unitary mode transformation  $U \in U(N)$  which yields the new modes  $\varphi'_i = \sum_j U_{ij} \varphi_j$ , the coefficient tensor  $C$  of a given fixed wavefunction  $\Psi$  transforms to  $C' = G(U)^\dagger C$  where  $G(U)$  is a unitary transformation on the space of many-body coefficient tensors.

For simplicity let us focus on the time reversal symmetric case, where  $C$  and the  $\varphi_i$  can be taken to be real-valued and mode transformations are given by an orthogonal matrix  $U \in O(N)$  or, discarding an immaterial overall sign factor,  $U \in SO(N)$ . Such matrices can be parametrized as  $U = e^A U_*$  with  $U_*$  an arbitrary fixed matrix in  $SO(N)$  and  $A$  real and skew-symmetric, the parametrization being unique for  $U$  close to  $U_*$ . Thus stationarity of a scalar function  $f$  on  $SO(N)$  at  $U_*$  is equivalent to

$$0 = \left. \frac{d}{dt} \right|_{t=0} f(e^{tA} U_*) = \text{Tr} \frac{\partial f}{\partial U}(U_*) U_*^T A^T, \quad \forall A^T = -A \quad (2)$$

that is to say  $\frac{\partial f}{\partial U}(U_*) U_*^T$  symmetric.

*Reduction to pairwise rotations:* We observe that to achieve stationarity it is sufficient to minimize  $f$  over all pairwise rotations  $U_{ij}(\theta)$  given by  $e^{\theta E_{ij}}$ ,  $E_{ij} = e_i e_j^T - e_j e_i^T$ , where  $e_i$  is the unit vector of  $\mathbb{R}^N$  whose  $i$ -th component is 1 and whose other components are zero. This corresponds to the mode transformation  $\varphi'_i = \cos \theta \varphi_i + \sin \theta \varphi_j$ ,  $\varphi'_j = -\sin \theta \varphi_i + \cos \theta \varphi_j$  which leaves all other modes the same. Indeed, if  $\left. \frac{d}{d\theta} f(U_{ij}(\theta) U_*) \right|_{\theta=0} = 0$  for all  $i < j$ , then the r.h.s. of (2) vanishes for all  $A = E_{ij}$ ; but since the  $E_{ij}$  span the space of skew matrices, it vanishes for all skew  $A$ .

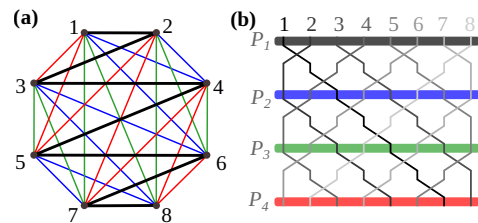


FIG. 1. (a) Walecki's construction [22] for  $N = 8$  modes. The modes are placed in a zig-zag line to the vertices of a regular polygon with  $N$  vertices ( $N$  is even). This thick black zig-zag line marks also the first permutation. Other permutations are generated by rotating the zig-zag line by the central angle of the regular polygon (blue, green, and red lines in figure). (b) Realization of permutations by swapping nearest neighbor modes in a checkerboard pattern. At every second layer of swap gates the next permutation of the construction in panel (a) is implemented. For better readability, we used the same colors to mark permutations in the two panels.

*Reduction to permutations and nearest neighbor rotations:* Next we observe that the set of all pairwise rotations  $U_{ij}(\theta)$  can be realized by  $N/2$  global re-orderings of the orbitals and the  $N-1$  nearest-neighbor rotations for each ordering. More precisely, if  $\tau_1, \dots, \tau_{N/2}$  are the specific permutations described further below such that any pair of orbitals become nearest neighbours under one of these permutations (that is, for all  $i < j$  there exist  $\nu$  and  $\ell$  such that  $\{\tau_\nu(i), \tau_\nu(j)\} = \{\ell, \ell + 1\}$ ), then

$$U_{ij}(\theta) = \tau_\nu^{-1} U_{\ell, \ell+1}(\pm\theta) \tau_\nu$$

with '+' if  $\tau_\nu(i) < \tau_\nu(j)$  and '-' otherwise.

The above construction is easily generalized to the general complex case, where  $U \in U(N)$ . The matrix  $A$  is then skew-hermitian, which is parameterized by  $N^2$  real numbers. The  $N$  purely imaginary diagonal elements of  $A$  do not change the value of  $f$  and can therefore be disregarded. The remaining  $N(N-1)$  parameters come again from two-mode rotations  $U_{ij}$  whose non diagonal elements are, however, parameterized by two real numbers (angles).

*Swap gates controlled permutations:* The optimal set of permutations  $\tau_1, \dots, \tau_{N/2}$  can be generated by Walecki's method [22] for even  $N$ 's, which has been originally developed to get the Hamiltonian decomposition of complete graphs. [23, 24]. In the construction, a regular polygon of  $N$  vertices is drawn and indices of the  $N$  modes are assigned to the vertices of the polygon using a zig-zag path (see Fig. 1). This zig-zag path corresponds to the first permutation,  $[1, 2, \dots, N]$ . Other permutations are generated by rotating the zig-zag path around the center of the polygon by the angle  $\frac{2\pi}{N}$ . It is easy to see that the  $\frac{N}{2}$  zig-zag lines cover all the edges of the complete graph of  $N$  vertices (modes) exactly once, i.e. every pair of modes is in nearest neighbor position once during the process. The same method with a minor modification can also be used to find optimal permutations for odd  $N$  values too. In this case the permutations are first generated

for  $N + 1$  modes, then the largest mode index ( $N + 1$ ) is simply erased from the permutations. We note that some mode pairs, however, are accessed more then once during the process for odd  $N$  values.

A pleasant feature of Walecki's method from the algorithmic point of view is the fact that consecutive permutations are easily generated by two layers of nearest neighbor swap operations placed in a checkerboard pattern. (see Fig. 1b). In the language of matrix product states, these swap operations can easily be executed by the elementary step of the time evolving block decimation (TEBD) algorithm [25], hence transforming the state vector between consecutive permutations is numerically cheap. This is equivalent to perform a full forward mode optimization sweep with fixed, but alternating angles of  $\pi/2$  and 0 and a backward sweep in a reversed order. In order to avoid truncation of the wavefunction, the bond dimension has to be increased by a factor of  $q$  for both the forward and the backward sweeps, where, in our case,  $q = 2$  is the local dimension of a fermionic mode. It is interesting to note, that neighbouring sites travel in opposite direction and they scatter back at the boundaries.

*Local mode optimization and block entropy area:* For a local mode optimization, the single particle unitary mode transformation  $U$ , under which Hamiltonian transforms as  $H(U) = G(U)^\dagger H G(U)$  is constructed iteratively from two-mode unitary operators by optimizing  $\theta_{l,l+1}$  while sweeping through the network for  $l = 1 \dots N - 1$  [12]. At each micro-iteration step, the half-Rényi block entropy  $S_{1/2}(\rho_{\{1,2,\dots,l\}})$  is minimized by a two-mode rotation, where  $\rho_{\{1,2,\dots,l\}}$  is the density operator of the first  $l$  modes. This local optimization procedure in general converge to a sub-optimal local minima, therefore a systematic global reordering of modes is necessary. In former works, this has been done by the Fiedler-vector method [12, 19]. This latter step provides a new set of pairwise  $\theta_{ij}$  components, but it does not traverse through systematically the full  $\theta_{ij}$  parameter space.

*Locality of the BEA:* For an iterative optimization protocol, where the global cost function is a sum of many local terms, it is usually also required for local optimization steps that they should change only the corresponding local term of the cost function. For the case of the BEA, it is easy to show that nearest neighbor rotations by  $\theta_{l,l+1}$  change only the block entropy measured when the cut is at mode  $l$ , while all other block entropies remain invariant. Consequently, the systematic decrease in the cost function BEA is ensured when only local, nearest neighbor rotations are considered. However, to access all the generators of the  $SU(N)$  one-particle rotation group one has to introduce long ranged two-mode rotations, or alternatively, apply a systematic reordering of the sites.

On the other hand, after the action of the swap gates there is a new ordering of the modes which changes the BEA. This leads to a new parameter regime for  $\theta_{ij}$  that is not connected to the original phase space by single orbital rotations as shown in Fig. 2(a). Therefore, for a precise mathematical treatment the BEA should be cal-

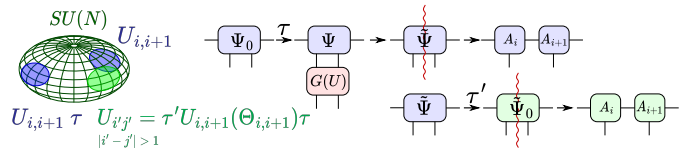


FIG. 2. (left) Schematic plot of the disconnected regions of the parameter space due to swap gate layer indicated by  $\tau$ . (right) Calculation of the cost function without and with inverse swap gates.

culated with respect to the original ordering. But this would require first permuting back the wave function via the inverse action of the swap gates as summarized in Fig. 2(b). More precisely, all layers of the swap gates must be executed in inverse order and the bond dimension should be increased by a factor of  $q^2$  for each layer to avoid additional truncation in the MPS wave function. Therefore, in the worst scenario each optimization step to get a new  $\theta_{l,l+1}$  would require  $N/2 - 1$  inverse swap gate layers and  $N - 1$  SVD step to recalculate the corresponding block entropy values with a systematic increase of the bond dimension. This would make the algorithm mathematically exact according to Eqs. 1- 2, but at the same time very costly. Therefore, we now present a more efficient protocol where the BEA is always measured for the actual permutation, where stationarity can still be achieved.

*Global DMRG-mode-optimization protocol:* In one macrostep, one first performs a  $N_{\text{SW}}^{\text{dmrg}}$  number of DMRG optimization sweeps, where the energy is optimized, then  $N_{\text{SW}}^{\text{opt}}$  local mode optimization sweeps as described above, where the BEA is optimized, and finally a swap-gate controlled permutation of the modes as described above to prepare the next macrostep. In order to reduce the harm may caused by the swap gates, truncation is avoided in this last step by allowing for a factor of  $q^2$  increase in the bond dimension. This increased bond dimension is, however, truncated back later. This macrostep is then repeated until convergence.

*Consistency:* As described below, our method is observed to converge after a moderate number of macrosteps. A preliminary theoretical explanation is based on the locality of the two swap gate layers, in the sense that they perform a sequence of nearest-neighbor permutations. Therefore subsequent application of several DMRG sweeps via nearest neighbor mode optimization can eliminate the perturbation induced by the swap layers. This is expected to happen once the algorithm has found the stationary solution for both energy and BEA.

*Numerical results:* Numerical simulations will be presented for a very general form of the Hamiltonian operator,

$$\mathcal{H} = \sum_{ij\alpha\beta} T_{ij}^{\alpha\beta} c_{i\alpha}^\dagger c_{j\beta} + \sum_{ijkl\alpha\beta\gamma\delta} V_{ijkl}^{\alpha\beta\gamma\delta} c_{i\alpha}^\dagger c_{j\beta}^\dagger c_{k\gamma} c_{l\delta}, \quad (3)$$

implemented in our code [26], that can treat any form of non-local interactions related to two-particle scattering processes. In Eq. 3  $i, j, k$  and  $l$  label the modes in the tensor network, while  $\alpha, \beta, \gamma$  and  $\delta$  denote spin indices. It can thus describe nuclear shell problems, or quantum chemistry even in the relativistic domain [6, 7, 27–40]. By proper choices of  $T_{ij}^{\alpha\beta}$  and  $V_{ijkl}^{\alpha\beta\gamma\delta}$  the Hamiltonian operator can also describe lattice models of fermions with local interactions and even models in two spatial dimensions with periodic boundary conditions are easily accessible [14, 16]. After mode optimization, however, the local nature of the Hamiltonian is lost and for the generic case the dimension of the matrix product operator (MPO) increases from  $\sqrt{N}$  to  $N^2$  [16]. Nevertheless, the overall computational complexity and wall time for a given error margin can be reduced by several order of magnitudes when mode optimized basis is utilized [16].

In the presented optimization protocol, starting with the natural ordering of modes from one to  $N$ , we traverse through all required permutations to generate all the  $\theta_{ij}$  pairs one or two times. Once the stationary point is reached, although the cost function is evaluated for different orderings, the reversal of the action of the swap gates is quickly achieved by the mode optimization, at low computational cost. This is due to the locality of the swap gates together with the smooth stationary entropy profile (see Fig. 4). In practice, at the end a number  $N_{\text{SW}}^{\text{opt,fin}}$  of final sweeps are performed using only local mode optimization.

In Fig. 3(a) the block entropy area is shown as function of DMRG sweep number for the  $6 \times 6$  spinless fermion model obtained with fixed  $D_{\text{opt}} = 80$  for 28 macro mode optimization cycles. In Fig. 3(b) the convergence of the ground state energy is presented for completeness. Here BEA  $\mathcal{B}_\alpha(C)$  is shown for  $\alpha = 1$ , as this is more commonly used in quantum many-body physics [41–44]. The tremendous drop in BEA is obvious from the figure. In the initialization phase, i.e., for the first  $N$  macro mode optimization cycles, however, the strict monotonicity was not enforced, thus all permutations have been generated. Therefore, BEA could increase after the MPS wave function is perturbed via the swap gates, but in practice in our simulations this was removed by the subsequent mode optimization steps. In addition, such unwanted effect also dies off via the optimization procedure as the wave function converges (see next paragraph). The DMRG-only six sweeping to recover the MPS wave function after the application of swap gates are included only for completeness, but these have no theoretical relevance, i.e., using only one forward and backward DMRG sweep with  $N_{\text{SW}}^{\text{dmrg}} = 2$  already generates a good starting wave function for the local mode optimization protocol. For further reference, we also show by solid black and red lines when optimization is performed on the MPS manifold only via DMRG and jointly together on the Grassman manifold via local mode optimization, but without global permutations, respectively. The convergence to highly sub-optimal solution is clearly seen, proving the

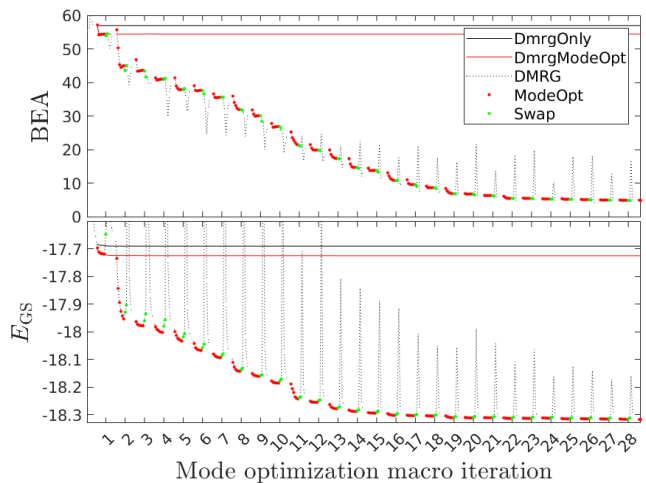


FIG. 3. (a) Block entropy area  $\mathcal{B}_1(C)$  and (b) ground state energy for the first 28 mode optimization macro iterations with  $D_{\text{opt}} = 80$ ,  $N_{\text{SW}}^{\text{dmrg}} = 6$ ,  $N_{\text{SW}}^{\text{opt}} = 6$ , and  $N_{\text{SW}}^{\text{opt,fin}} = 6$  for the  $6 \times 6$  spinless model. Dashed line indicates data point obtained via DMRG, red dot refers to mode optimization and green dot to application of swap gates. End of each mode optimization macro cycle corresponds to every subsequent green symbols. After 36 mode optimization macro iterations another six mode optimization macro iterations are performed without utilizing swap gates for completeness (not shown). For further reference, solid black and red lines show results obtained by DMRG only and by DMRG together with mode optimization, but without swap gate controlled permutation, respectively.

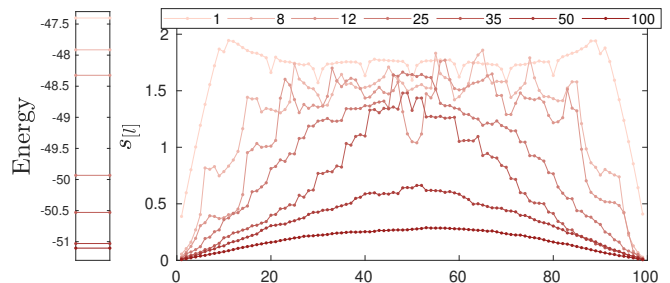


FIG. 4. Ground state energy (left) and block entropy,  $s[l]$ , as a function of the left block size,  $l$  (right) for some selected mode transformation macro iteration cycles 1, 8, 12, 25, 35, 50, 100, with fixed bond dimension  $D_{\text{mo}} = 80$  and 11 sweeps for the half-filled  $10 \times 10$  two-dimensional spinless fermionic model with model parameters given in Ref. [16]. The area under each curve corresponds to the block entropy area  $\mathcal{B}_1(C)$  shown in Fig. 3. Note that a full iteration to bring each mode to be neighbours at least once contains  $N/2 = 50$  permutations, i.e., 50 mode transformation macro iterations.

importance of permutations.

Repeating our procedure for larger system sizes, i.e., for  $n = 8, 10, 12$ , we obtained similar stable and robust behavior. In Fig. 4 we present the ground state energy (left) and block entropy as a function of the left block size,  $l$  (right) for some selected mode transformation macro

iterations for the  $10 \times 10$  spinless fermion model using the same algorithmic settings as discussed above. We highlight the very symmetric block entropy profile of the optimized modes, that resulted without any specific ordering procedure, unlike our previous attempts based on the Fiedler vector approach [19]. This profile also resembles those of one dimensional local models [42, 43]. In addition, the new approach does not require the calculation of two-mode correlation functions [45] to obtain two-mode mutual information which leads to a significant speedup. Furthermore, since the perturbation on the wave function via the swap gates preserves locality it can get suppressed as the block entropy profile converges since only sites with very similar site entropy values get mixed in a window of five sites. This also makes it possible to continue the optimization procedure with a new permutation and does not require a full restart like in our previous approach based on the Fiedler vector [12]. We also experienced that the Fiedler vector based approach, although converging faster for the first few macro iterations steps by bringing the most important modes next to each other, does not guarantee a monotonic decrease of BEA. Instead, the BEA and the energy start to oscillate for further iteration steps. In contrast to this, our new approach converges systematically, usually generates an even better optimized basis after  $N$  mode transformation macro iterations, and can eliminate the perturbation of the swap layers once the stationary point is reached. Therefore a lower number of sweeps is required for reaching convergence, reducing the total computational complexity and wall time of the mode optimization protocol. In practice to boost convergence, first a few mode optimization macro iterations can be performed via the Fiedler vector approach which is followed by the systematic refinement of the modes via the new swap-gate controlled permutation protocol. Applying our procedure to strongly correlated molecular systems studied in Refs. [12, 15, 46] we reproduced the

previous results, but in a fraction of computational time.

*Conclusion:* In this work, we proposed a general approach to find an optimal representation of a quantum many body wave function via global fermionic mode optimization. The stationary point on a fixed rank matrix product state manifold is obtained via a joint optimization on the Grassman manifold together with swap gates controlled permutations to generate the whole unitary group parametrized by one particle basis rotations. The minimization of the global quantity, the block entropy area, guarantees that the method fulfills all criteria with respect to partial derivatives. Numerical results via large scale density matrix renormalization group simulations on strongly correlated molecular systems and two-dimensional fermionic lattice model are discussed. The new protocol is very robust, the convergence is guaranteed by construction and numerically much cheaper than previous attempts.

*Acknowledgments:* This work has been supported by the Hungarian National Research, Development and Innovation Office (NKFIH) through Grant Nos. K134983 and TKP2021-NVA-04, by the Quantum Information National Laboratory of Hungary. Ö.L. acknowledges financial support by the Hans Fischer Senior Fellowship programme funded by the Technical University of Munich – Institute for Advanced Study and by the Center for Scalable and Predictive methods for Excitation and Correlated phenomena (SPEC), funded as part of the Computational Chemical Sciences Program FWP 70942 by the U.S. Department of Energy (DOE), Office of Science, Office of Basic Energy Sciences, Division of Chemical Sciences, Geosciences, and Biosciences at Pacific Northwest National Laboratory. M.A.W. has also been supported by the Janos Bolyai Research Scholarship of the Hungarian Academy of Sciences. The simulations were performed on the national supercomputer HPE Apollo Hawk at the High Performance Computing Center Stuttgart (HLRS) under the grant number MPTNS/44246.

- 
- [1] R. J. Bartlett and M. Musiał, *Reviews of Modern Physics* **79**, 291 (2007).
  - [2] G. Carleo and M. Troyer, *Science* **355**, 602 (2017).
  - [3] A. Nagy and V. Savona, *Physical Review Letters* **122**, 250501 (2019).
  - [4] F. A. Evangelista, G. K. Chan, and G. E. Scuseria, *The Journal of Chemical Physics* **151** (2019), <https://doi.org/10.1063/1.5133059>.
  - [5] K. Choo, A. Mezzacapo, and G. Carleo, *Nature Communications* **11**, 2368 (2020).
  - [6] U. Schollwöck, *Rev. Mod. Phys.* **77**, 259 (2005).
  - [7] U. Schollwöck, *Annals of Physics* **326**, 96 (2011), January 2011 Special Issue.
  - [8] F. Verstraete, T. Nishino, U. Schollwöck, M. C. Bañuls, G. K. Chan, and M. E. Stoudenmire, *Nature Reviews Physics*, 1 (2023).
  - [9] R. Orús, *Nature Reviews Physics* **1**, 538 (2019).
  - [10] S. R. White and R. M. Noack, *Phys. Rev. Lett.* **68**, 3487 (1992).
  - [11] V. Murg, F. Verstraete, Ö. Legeza, and R. M. Noack, *Phys. Rev. B* **82**, 205105 (2010).
  - [12] C. Krumnow, L. Veis, Ö. Legeza, and J. Eisert, *Phys. Rev. Lett.* **117**, 210402 (2016).
  - [13] C. Krumnow, Ö. Legeza, and J. Eisert, *arXiv [cond-mat.stat-mech]*, 1904.11999 (2019).
  - [14] C. Krumnow, L. Veis, J. Eisert, and Ö. Legeza, *Phys. Rev. B* **104**, 075137 (2021).
  - [15] M. Máté, K. Petrov, S. Szalay, and Ö. Legeza, *Journal of Mathematical Chemistry* (2022), 10.1007/s10910-022-01379-y.
  - [16] A. Menczer, K. Kapás, M. A. Werner, and Ö. Legeza, *Phys. Rev. B* **109**, 195148 (2024).
  - [17] J. Eisert, M. Cramer, and M. B. Plenio, *Rev. Mod. Phys.* **82**, 277 (2010).



- [18] E. M. Stoudenmire and S. R. White, *Annual Review of Condensed Matter Physics* **3**, 111 (2012).
- [19] G. Barcza, Ö. Legeza, K. H. Marti, and M. Reiher, *Phys. Rev. A* **83**, 012508 (2011).
- [20] D. Zgid and M. Nooijen, *The Journal of Chemical Physics* **128**, 144116 (2008).
- [21] A. Menczer, Á. Ganyecz, M. A. Werner, J. Hammond, M. Ganahl, F. Neese, and Ö. Legeza, unpublished (2024), unpublished.
- [22] É. Lucas, *Récréations Mathématiques*, Vol. 1 (Gauthier-Villars, 1882).
- [23] J.-C. Bermond, in *Annals of Discrete Mathematics*, Vol. 3 (Elsevier, 1978) pp. 21–28.
- [24] R. J. Wilson, *Introduction to Graph Theory* (Addison Wesley Longman Ltd., Harlow, England, 1996).
- [25] G. Vidal, *Physical Review Letters* **91**, 147902 (2003).
- [26] Ö. Legeza, L. Veis, and T. Mosoni, “DMRG-Budapest, a program for condensed matter, quantum chemical, and nuclear shell DMRG calculations,” (2023).
- [27] S. R. White, *Phys. Rev. Lett.* **69**, 2863 (1992).
- [28] T. Xiang, *Phys. Rev. B* **53**, R10445 (1996).
- [29] S. R. White and R. L. Martin, *The Journal of Chemical Physics* **110**, 4127 (1999), <https://doi.org/10.1063/1.478295>.
- [30] R. M. Noack and S. R. Manmana, in *AIP Conference Proceedings* (AIP, 2005).
- [31] G. K.-L. Chan, J. J. Dorando, D. Ghosh, J. Hachmann, E. Neuscamman, H. Wang, and T. Yanai, in *Frontiers in Quantum Systems in Chemistry and Physics*, Progress in Theoretical Chemistry and Physics, Vol. 18, edited by S. Wilson, P. J. Grout, J. Maruani, G. Delgado-Barrio, and P. Piecuch (Springer, Netherlands, 2008).
- [32] S. Knecht, Ö. Legeza, and M. Reiher, *The Journal of Chemical Physics* **140**, 041101 (2014).
- [33] J. Dukelsky and S. Pittel, *Reports on Progress in Physics* **67**, 513 (2004).
- [34] R. Orús, *Annals of Physics* **349**, 117 (2014).
- [35] Ö. Legeza, L. Veis, A. Poves, and J. Dukelsky, *Phys. Rev. C* **92**, 051303 (2015).
- [36] Sz. Szalay, M. Pfeffer, V. Murg, G. Barcza, F. Verstraete, R. Schneider, and Ö. Legeza, *Int. J. Quantum Chem.* **115**, 1342 (2015).
- [37] Ö. Legeza and C. Schilling, *Phys. Rev. A* **97**, 052105 (2018).
- [38] I. Shapir, A. Hamo, S. Pecker, C. P. Moca, Ö. Legeza, G. Zarand, and S. Ilani, *Science* **364**, 870 (2019), <https://www.science.org/doi/pdf/10.1126/science.aat0905>.
- [39] G. Barcza, V. Ivády, T. Szilvási, M. Vörös, L. Veis, Á. Gali, and Ö. Legeza, *Journal of Chemical Theory and Computation* **17**, 1143 (2021), pMID: 33435672, <https://doi.org/10.1021/acs.jctc.0c00809>.
- [40] A. Baiardi and M. Reiher, *The Journal of Chemical Physics* **152**, 040903 (2020), <https://doi.org/10.1063/1.5129672>.
- [41] G. Vidal, J. I. Latorre, E. Rico, and A. Kitaev, *Physical review letters* **90**, 227902 (2003).
- [42] P. Calabrese and J. Cardy, *Journal of Statistical Mechanics: Theory and Experiment* **2004**, P06002 (2004).
- [43] Ö. Legeza, J. Sólyom, L. Tincani, and R. M. Noack, *Physical Review Letters* **99**, 087203 (2007).
- [44] L. Amico, R. Fazio, A. Osterloh, and V. Vedral, *Rev. Mod. Phys.* **80**, 517 (2008).
- [45] G. Barcza, R. M. Noack, J. Sólyom, and O. Legeza, *Phys. Rev. B* **92**, 125140 (2015).
- [46] K. Petrov, A. Ganyecz, Z. Benedek, A. Olasz, G. Barcza, and Ö. Legeza, in *Advances in Methods and Applications of Quantum Systems in Chemistry, Physics, and Biology Selected Proceedings of QSCP-XXV Conference (Torun, Poland, June 2022)*, edited by I. Grabowski, K. Słowik, J. Maruani, and E. J. Brändas (Springer, Cham, 2024).